ACS OMEGA

http://pubs.acs.org/journal/acsodf

Article

Coil Formation of a Silicone String Using UV−Ozone Treatment

Masashi Watanabe,* Toshiki Tokutake, Ai Harada, and Masatoshi Kaminaga

Cite This: *ACS Omega* 2022, 7, 11363−11370

Read Online

ACCESS | Metrics & More | Article Recommendations | Supporting Information

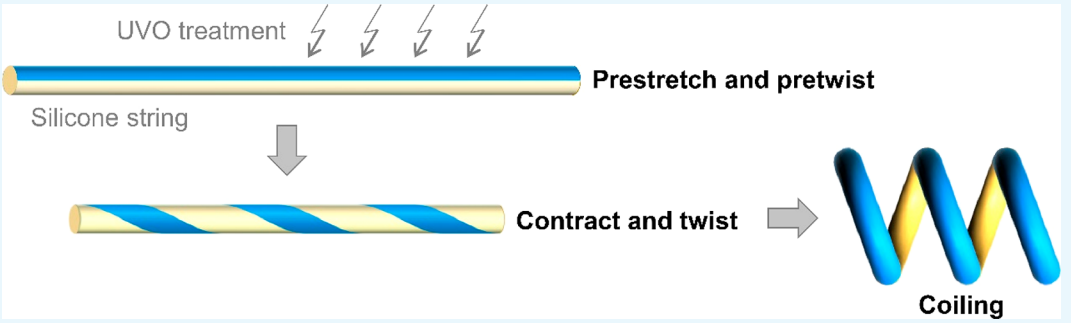

ABSTRACT: Microcoils are used in various mechanical devices. However, existing methods for producing microcoils from polymers often require expensive equipment. In this study, microcoils were prepared using a cost-effective and simple method. The material used was silicone, which is a biocompatible polymeric material. Silicone was solidified inside glass capillaries to form thin, straight strings with a diameter of 140 μm. The string was then transformed to a coil shape by oxidation using UV−ozone treatment while it was prestretched and pretwisted. The resilience force from the prestretching and pretwisting forces caused the string to bend and twist, respectively. As a result of the combination of these deformation modes, a coil was formed. As an application of the coils, an actuator was prepared, which repeatedly transforms between straight and coiled shapes. The actuation was caused by the swelling/deswelling of silicone with hexane. A large strain of 54% was obtained.

INTRODUCTION

Coil springs can be easily stretched, compressed, bent, and twisted, even if the wire is made of a stiff material. This unique property of the coils can be attributed to their configuration. Therefore, small coils, i.e., on the order of millimeters to nanometers, are widely used as springs,[1] actuators,[2,3] flow sensors,[4] strain sensors,[5] stretchable interconnects,[6] electromagnetic absorbers,[7] and artery embolization materials,[8] among others. The materials used for the wire of such coils include metals,[9] inorganic materials such as silicon[10] and carbon,[11] synthetic polymers,[12] biopolymers such as DNA,[13] and even organism such as algae.[14] Therefore, methods for producing microcoils vary widely.

The methods for producing microcoils made of synthetic polymers also vary. Two-photon polymerization is an example of such a method; however, the apparatus needed for this method is costly.[15] If sodium alginate is used as the polymeric material, wet spinning using microfluidic channels[16] or syringe needles[17] is a relatively cost-effective method for obtaining coiled fibers. Melt spinning is also used to produce coil-shaped fibers using the difference in coefficients of the thermal expansion between two polymers. Polymers with similar viscosities and melting points must be selected in this method.[18] Polymers molded into ribbon-like strips can roll up to form a helical structure if the strip has a diagonal striped pattern. This method incurs the cost of photomasks.[19]

Silicones, i.e., polydimethylsiloxane (PDMS) and its derivatives, are soft and highly biocompatible. Therefore, they are promising for the biomedical applications of microcoils. Three-dimensional silicone microstructures can be produced using digital laser engraving[20] and laser direct writing.[21] However, these methods require expensive equipment. In this study, we developed a cost-effective process for producing silicone microcoils through molding in glass capillaries and UV−ozone treatment. The surface of a PDMS sheet can be oxidized by UV−ozone treatment[22] or chemical treatment[23] to form a silica-like hard layer. If the sheet is prestretched, then its contraction after the treatment induces wrinkles because the surface layer is less elastic than the underlying PDMS sheet.[24] Therefore, in this study, a similar method was applied to PDMS strings to form a coil shape. Furthermore, actuators were prepared using the transformation between the coil and straight shapes.

Received: January 24, 2022
Accepted: March 9, 2022
Published: March 21, 2022

EXPERIMENT

Materials. Glass capillaries were purchased from Hirschmann Laborgeräte (Eberstadt, Germany). The inner diameter and length were 0.14 and 32 mm, respectively. Silicone prepolymer (KE-103) and curing agent (CAT-103) were acquired from Shin-Etsu Chemical (Tokyo, Japan). Zinc oxide power (particle size: up to 5 μm), 1,1,1,3,3,3-hexamethyldisilazane (HMDS), 3-aminopropyltrimethoxysilane (APTMS), and brilliant blue FCF were obtained from Fujifilm Wako Pure Chemical (Osaka, Japan).

Preparation of Silicone Strings. The silicone prepolymer (KE-103), curing agent (CAT-103), and zinc oxide powder were mixed together in a mass ratio of 100:5:20. Zinc oxide powder was used to make the transparent silicone white in order to facilitate optical microscope observations. This mixture was degassed under vacuum. Glass capillaries, which were pretreated with HMDS vapor at room temperature for 3 days, were placed in an aluminum foil cup, into which the mixture was poured and degassed again under vacuum for 30 min (Figure 1a). After the cup was stored at room temperature for 3 days to solidify the mixture, it was immersed in acetone for 2 h to soften the solidified silicone. The capillaries were collected by removing the silicone attached outside the capillaries. The silicone inside the capillary, which slightly protruded from the end of the capillary due to swelling with acetone (Figure 1b), was drawn out using tweezers. To make this process easier, drawing was carried out while the capillary was soaked in methanol. The obtained silicone string, whose diameter and length were 0.14 and 32 mm, respectively, was dried in air at room temperature (Figure 1c).

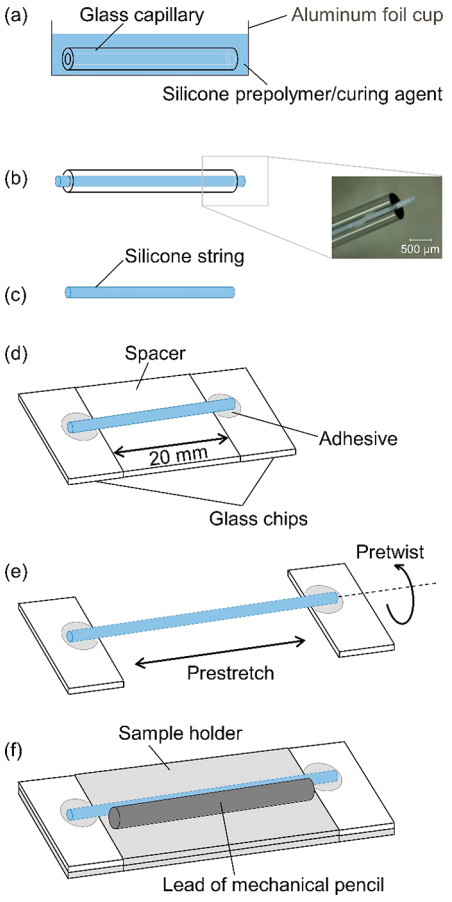

Figure 1. Experimental procedure for preparing silicone coils. (a) Silicone prepolymer was solidified in a cup made of aluminum foil with a capillary. (b) Silicone inside the capillary was swollen with acetone. (c) A silicone string was drawn out of the capillary. It was (d) fixed on glass chips and (e) prestretched and pretwisted before UV−ozone treatment. (f) While one side of the string was masked with lead from a mechanical pencil, the string was oxidized using UV−ozone treatment and finally released from the glass chips to form a coil.

Production of Silicone Coils via UV−Ozone Treatment. Two glass chips and a spacer were prepared from glass slides. The glass slide surfaces were roughened using an abrasive (Fuji white alumina WA220; Fuji Manufacturing, Tokyo, Japan) because the silicone strings tend to stick to smooth surfaces (Figure 1d). To straighten the silicone string, it was carefully placed on two aligned chips and a spacer (Figure S1a, Supporting Information). Both ends of the string were fixed to the chips using an adhesive. Before the UV−ozone treatment, the string was prestretched and pretwisted (Figure 1e). The stretching ratio $(l - l_0)/l_0$ was 0.75, where l_0 and l are the original and stretched string lengths, respectively (Figure S1b). The string was pretwisted clockwise (typically three times), which meant that the string would be twisted counterclockwise by the resilience force of the material after the string was released. As shown in Figure 1f, the glass chips were fixed on a sample holder, and lead from a mechanical pencil (0.3 mm thickness, C273-HB, Pentel, Tokyo, Japan) was attached to the string using a small amount of starch paste to mask one side of the string during the UV−ozone treatment (Figure S1c).

The UV−ozone treatment was carried out for 90 min using a UV−ozone cleaner (PC440, Meiwafosis, Tokyo, Japan). The sample holder was then immersed in water to remove the lead by solvating the starch paste. The string was removed from the holder by cutting both ends of the string, which meant that the string was released from prestretching and pretwisting. Thus, a coil was formed.

Staining of the Oxidized Portion of the Silicone Coil. The silicone coil was immersed in a mixture of APTMS, methanol, and distilled water in a mass ratio of 2:20:1 at room temperature for 20 min and then washed with methanol.[25] It was then soaked in a solution of a blue dye (brilliant blue FCF, methanol, and 1 M hydrochloric acid in a mass ratio of 1:400:1) at room temperature for 20 min, washed with methanol, and dried in air. Only the portion oxidized by the UV−ozone treatment was stained blue.

Microscopic Observation of the Silicone Coils. The coils were observed using a digital microscope (VHS-2000, Keyence, Osaka, Japan).

GEOMETRICAL CONSIDERATION

A coil wrapping an n-gonal prism is considered. Figure 2a shows the case when $n = 6$. The diameter and pitch are $2a$ and p, respectively. To produce the coil, a straight string is first bent at equally spaced points at the same bending angle, θ, followed by twisting around each side with the same torsion angle φ (Figure 2b). The spacing, e.g., A′B′, is the same as the length AB along the coil:

$$\mathrm{AB} = \sqrt{4a^2\left(\sin\frac{\pi}{n}\right)^2 + \left(\frac{p}{n}\right)^2} = \mathrm{A'B'} = \mathrm{B'C'} = \ldots \quad (1)$$

https://doi.org/10.1021/acsomega.2c00475
ACS Omega 2022, 7, 11363−11370

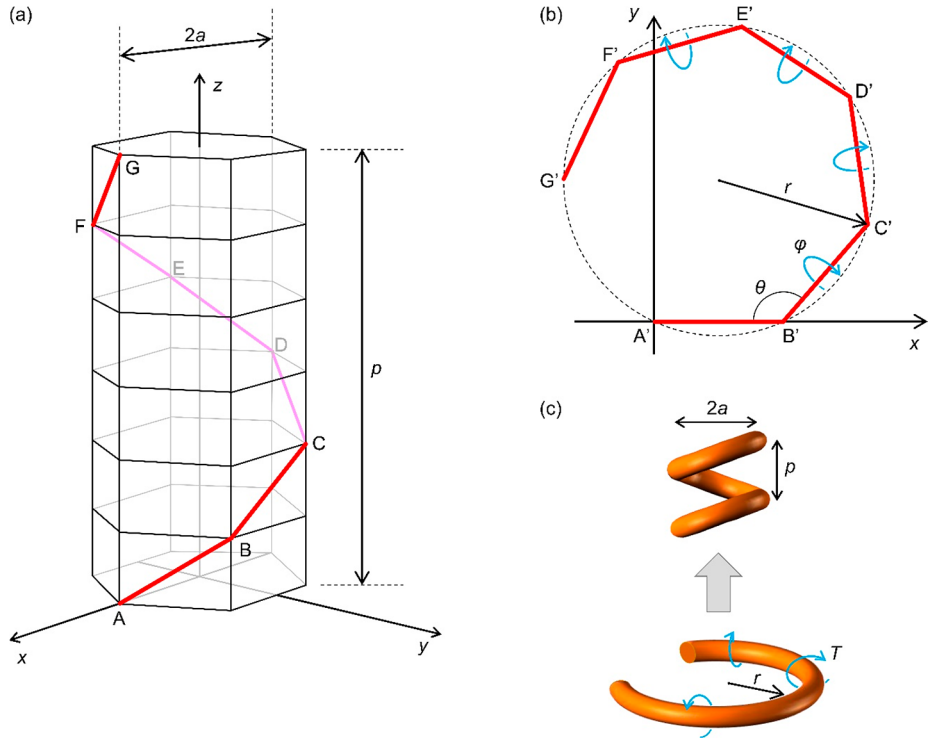

Figure 2. Theoretical model of coil formation. (a) The string shown as a red line wraps an n-gonal prism ($n = 6$). (b) The string is first bent at equally spaced points, followed by twisting around each side to form a coil. (c) The curved string forms a coil by being twisted ($n = \infty$).

The bending angle ∠A′B′C′ is the same as the angle ∠ABC along the coil:

$$\theta = \angle A'B'C' = \angle ABC = \cos^{-1}\left\{\frac{-4a^2\left(\sin\frac{\pi}{n}\right)^2\left(\cos\frac{2\pi}{n}\right) - \left(\frac{p}{n}\right)^2}{4a^2\left(\sin\frac{\pi}{n}\right)^2 + \left(\frac{p}{n}\right)^2}\right\} \quad (2)$$

The torsion angle, such as the angle around BC, is expressed as follows because it is the same as the angle formed by normal vectors of the plane containing A, B, and C and the plane containing B, C, and D:

$$\varphi = \cos^{-1}\left\{\frac{\left(\frac{p}{n}\right)^2\cos\frac{2\pi}{n} + a^2\left(\sin\frac{2\pi}{n}\right)^2}{\left(\frac{p}{n}\right)^2 + a^2\left(\sin\frac{2\pi}{n}\right)^2}\right\} \quad (3)$$

When n tends to infinity, the twist angle per unit length T is expressed as

$$T = \lim_{n\to\infty}\frac{\varphi}{AB} = \frac{2\pi p}{(2\pi a)^2 + p^2} \quad (4)$$

When n tends to infinity, the radius r of the circle passing through A′, B′, and C′ is written as

$$r = \lim_{n\to\infty}\frac{A'B'}{2\cos\frac{\theta}{2}} = a\left\{1 + \left(\frac{p}{2\pi a}\right)^2\right\} \quad (5)$$

From eqs 4 and 5, the following equations are obtained:

$$a = \frac{r}{1 + r^2T^2} \quad (6)$$

$$p = \frac{2\pi r^2 T}{1 + r^2T^2} \quad (7)$$

Therefore, when a coil is produced by twisting a curved string (Figure 2c), the radius and pitch are predicted using eqs 6 and 7.

RESULTS AND DISCUSSION

Formation of Coils. UV−ozone treatment oxidizes the surface of silicone elastomers and forms a thin silica-like layer.[22] The lamp of UV−ozone cleaners typically emits light of two wavelengths, i.e., 185 and 245 nm. The 185 nm light generates ozone from the oxygen in the air, whereas the 254 nm light decomposes the generated ozone.[26] Atomic oxygen, which can effectively oxidize the silicone, is generated as an intermediate during both the formation and decomposition processes. UV light at 185 and/or 245 nm also dissociates chemical bonds in the silicone. These effects generate a silica-like material that is less elastic than the underlying unmodified silicone. Therefore, if a silicone film is stretched during the UV−ozone treatment and is thick enough, wrinkles form on the surface by removing the stretching. However, if the film is thin, it will bend after the release for the same reason.

The silicone string prepared in this study was thin (0.14 mm in diameter). During the UV−ozone treatment, the string was prestretched, and the lead of a mechanical pencil was glued to one side of the string to protect it from oxidation. After the UV−ozone treatment, the string was released from the prestretching and stained blue on the oxidized portion of the surface. The UV−ozone treatment bent the string facing the oxidized portion outward (Figure 3a−d), as expected owing to the less elastic nature of the oxidized surface.. Note that in this case the string is not pretwisted.

https://doi.org/10.1021/acsomega.2c00475
ACS Omega 2022, 7, 11363−11370

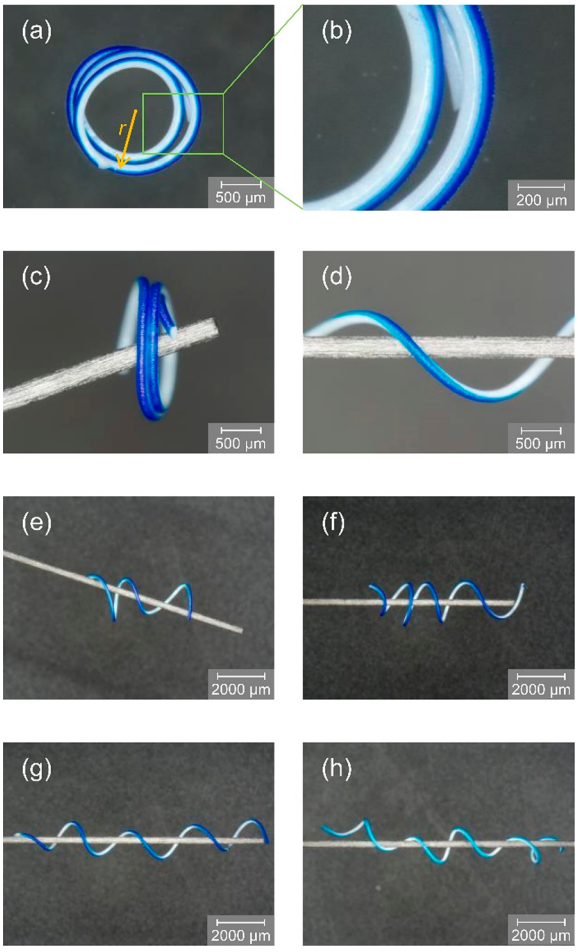

Figure 3. Optical images of coils whose oxidized portion was stained blue. The UV−ozone treatment was performed (a−c) without and (d) with pretwisting [(a and b) top view; (c) side view]. The pretwisting angles per unit length (rad cm^{-1}) were varied as (e) π, (f) 2π, (g) 3π, and (h) 4π.

The staining mechanism can be explained as follows. Because of the UV−ozone treatment, silanol groups are generated on the silicone surface,[27] and APTMS reacts with them. The amino groups of APTMS can act as adsorption sites for the acid dye (brilliant blue FCF). Thus, only the oxidized portion was stained.

When the strings were prestretched and pretwisted before the UV−ozone treatment, coils were formed during the release after the treatment (Figure 3e−h). The oxidized portion of these coils faced outward in all cases. The coil formation mechanism is schematically illustrated in Figure 4. One side of the prestretched and pretwisted silicone string was oxidized using UV−ozone treatment (Figure 4a−c). As described in the Geometrical Consideration section, both bending and twisting are needed to form a coil. As shown in Figure 4d, bending is caused by shrinkage from releasing the string. Simultaneously, twisting is induced by the resilience force from the pretwisting. If the pretwisting is clockwise, the twisting is counterclockwise. As a result of bending and twisting, the string formed a coil shape (Figure 4e).

The twist angle per unit length T_{twist}, which was calculated from the radius and pitch of the obtained coils using eq 4, was plotted against the pretwist angle per unit length $T_{pretwist}$ (Figure 5, line (a)). T_{twist} was slightly smaller than $T_{pretwist}$. The factor f, defined as $T_{twist}/T_{pretwist}$, was 0.88, suggesting that the shear strain caused by the pretwisting was not completely removed by the release because the oxidized portion comprised a silica-like rigid material.

On the basis of the geometrical consideration of coil formation, the coil radius a and pitch p can be predicted using the radius of curvature r of the curved string prepared without pretwisting (Figure 3a). From eqs 6 and 7, a and p were calculated and compared with those of coils actually prepared (Figure 3c,e−h). Here, T_{twist} was obtained by multiplying $T_{pretwist}$, which was calculated on the basis of the times of actual pretwisting by the factor ($f = 0.88$). As shown in Figure 6a,b, a and p were roughly consistent with the prediction. Measured values of a and p are scattered because the gluing of the lead to the silicone string was likely inhomogeneous. However, we can speculate that the accuracy of the masking was not poor on the basis of the microscope images of the side view of the coils (Figure 3e−h). In every figure, the area of the inside surface of the coils is only white whereas that of the outside surface is only blue, indicating that half of the surface was oxidized in every experiment.

When the lead was not used during the UV−ozone treatment, coils with a more homogeneous pitch and radius were obtained (Figure 7). The factor f was 0.51 (Figure 5, line (b)), indicating that approximately half of the pretwisting strain remained in the coil. The atomic oxygen generated during the UV−ozone treatment migrated to the back side of the silicone string and oxidized its surface to some extent, which was confirmed by staining the coils. Because both the front and back sides of the string were oxidized and thus hardened, the resilience from the pretwisting was incomplete. The pitch and radius of the coils were predicted from T_{twist} and r using eqs 6 and 7 (Figure 6c,d), which seem to be roughly consistent with the dimensions of the experimentally obtained coils. As these equations show, the prediction is sensitively dependent on r, and the inaccuracy of the measured r could be responsible for the difference between the prediction and the actual measurements.

The effect of the diameter of the silicone strings on the radius a and the pitch p of the coils was explored (Figure S2, Supporting Information). When the pretwist angle (3π rad cm^{-1}) and the duration of the UV−ozone treatment (90 min) were constant, both the radius and the pitch increased with the diameter. The reason these results were obtained can be explained as follows: As mentioned previously, the lower elasticity of the UV−ozone-treated surface layer, compared with that of the untreated foundation, causes bending of the string. Therefore, when a string with a larger diameter is used, the contribution of the surface layer is smaller, resulting in a smaller bending curvature. This means that the radius of curvature r in eqs 6 and 7 increases with the diameter. Because r^2T^2 was considerably smaller than 1 under the conditions used for preparing the coils, if approximation $1 + r^2T^2 \approx 1$ holds, then these equations predict that a and p increase with the diameter, which is consistent with the experimental results.

The effect of the duration of the UV−ozone treatment was also explored (Figure S3, Supporting Information). Considering that this duration would affect both the radius and the pitch in a complicated manner, the coils should be prepared without pretwisting so that the pitch can be neglected (theoretically $p = 0$, see eq 7). The results demonstrate that the bending curvature increased with the duration, suggesting

https://doi.org/10.1021/acsomega.2c00475
ACS Omega 2022, 7, 11363−11370

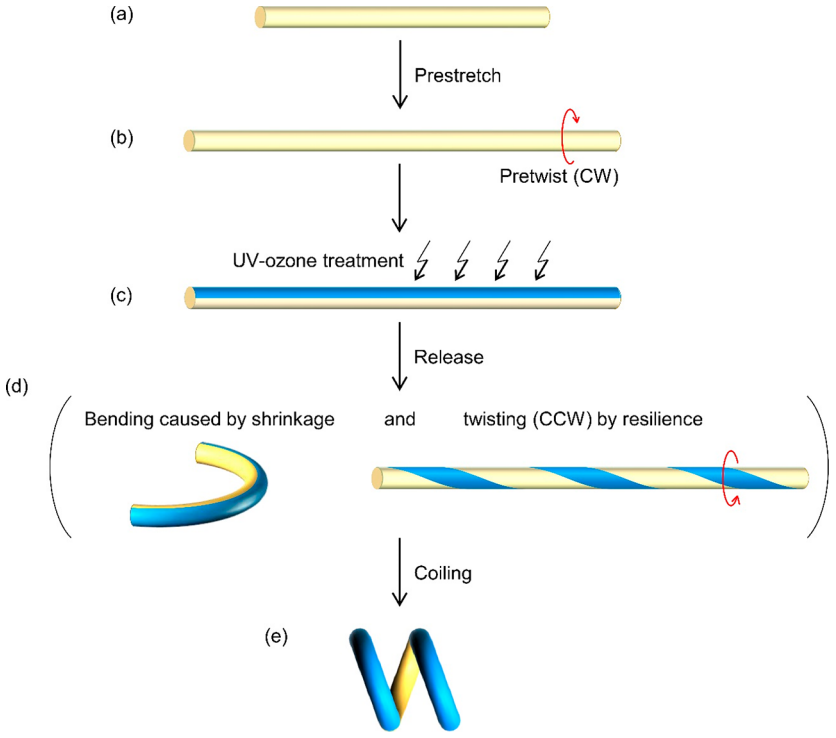

Figure 4. Schematic of the mechanism of coil formation using UV−ozone treatment. The silicone string is (a) prestretched, (b) pretwisted clockwise, and (c) one side of the string is oxidized using UV−ozone treatment. (d) By releasing the string from the prestretch and the pretwist, it shrinks and bends with the oxidized portion facing outward. Simultaneously, it twists counterclockwise owing to the resilience of the prestretch. (e) As a result of the bending and twisting, the string forms a coil shape.

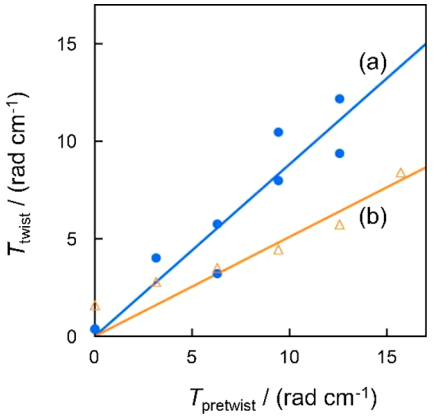

Figure 5. Relationship between the pretwist and twist angles per unit length, $T_{pretwist}$ and T_{twist}. During the UV−ozone treatment: (a) lead from a mechanical pencil as a mask was glued to the silicone string and (b) no masks were used.

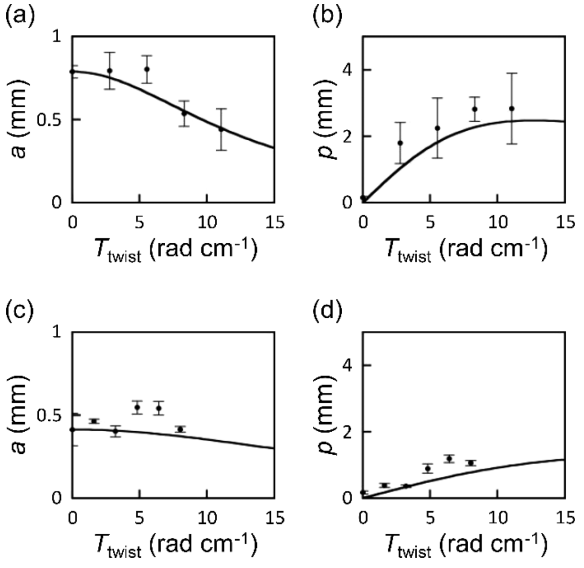

Figure 6. (a and c) Coil radius a and (b and d) coil pitch p plotted against twist angle T_{twist}. The solid lines show values calculated on the basis of eqs 6 and 7. For (a) and (b), the prepared coils are shown in Figure 3. For (c) and (d), they are shown in Figure 7. The error bars represent the standard deviations.

that the oxidized layer became thicker and/or harder. Thus, the curvature was controlled by varying the duration.

In the above studies, zinc oxide powder was added to silicone to obtain white coils, which were easy to observe using optical microscopy. The addition of zinc oxide powder did not significantly affect the radius and pitch of the silicone coils, as shown in the data obtained using transparent coils (Figure S4, Supporting Information).

The method for preparing the silicone coils is also applicable to polyurethane. A polyurethane elastomer string (~40 μm in diameter, Operon, purchased from CENFILL, Kumamoto, Japan) was prestretched (75%) and pretwisted (3π rad cm^{-1}), followed by UV−ozone treatment for 90 min to obtain a coil (Figure S5, Supporting Information). The treatment seemed to cause polyurethane to lose elasticity; nevertheless, we are now planning to explore the chemical aspects of the treatment and the mechanism of coiling.

Application of Silicone Coils as Actuators. The basic properties of the silicone coils as actuators were measured. The actuation mechanism utilized the swelling of the silicone with

https://doi.org/10.1021/acsomega.2c00475
ACS Omega 2022, 7, 11363−11370

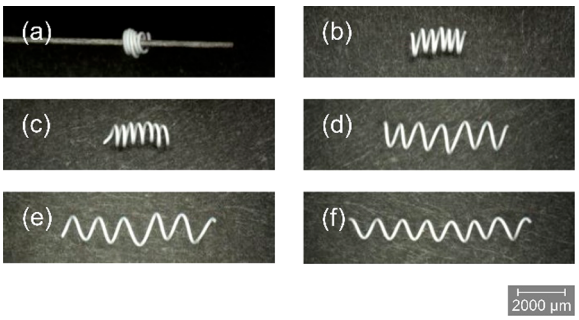

Figure 7. Optical images of coils prepared using the UV−ozone treatment without masks. The pretwist angles per unit length are (a) 0, (b) π, (c) 2π, (d) 3π, (e) 4π, and (f) 5π (rad cm^{-1}).

hexane. The coil (original length L_{air}) was stretched when immersed in hexane (stretched length L_{hex}) (Figure 8a).

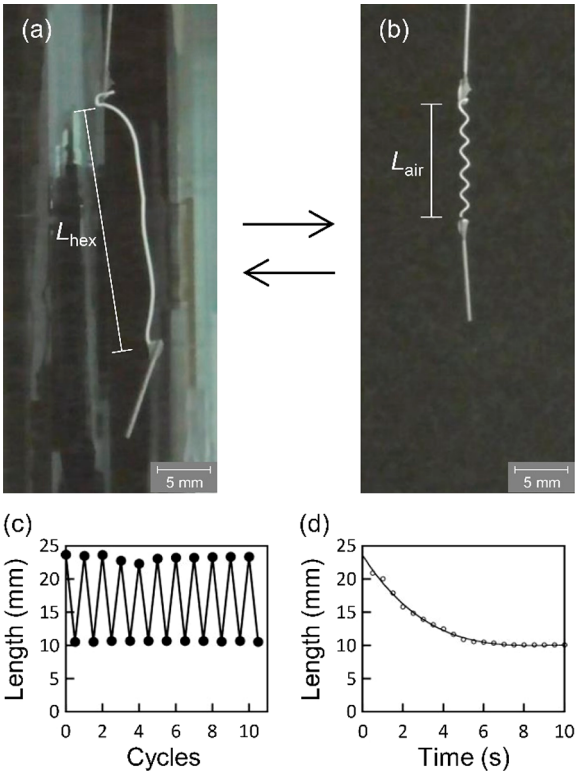

Figure 8. Silicone string in (a) hexane and (b) air. Change in length of the string (c) when the string was repeatedly moved between the hexane and air environments and (d) when the string swollen with hexane was moved to the air environment.

However, the original coil shape was recovered by placing the coil in air (Figure 8b). The strain during contraction [$(L_{hex} - L_{air})/L_{hex}$] was 54%. The actuator had a coil shape, which was responsible for the apparent large strain. The stretching and coiling of the actuator could be repeated more than 10 times without a significant decrease in strain (Figure 8c). The response time was ∼7 s (Figure 8d), which was relatively quick in comparison with typical hydrogel actuators which use the volume change between swelling and deswelling because the silicone string was very thin (0.14 mm in diameter).[28] The mass of the coil was ∼0.8 mg, and the weight attached at the bottom end was 1.9 mg. Thus, the actuator could lift a weight of more than twice its own weight. Similar actuation was also observed without the weight, although measuring the coil length in hexane became more time-consuming because the actuator floated for a long time in hexane.

Table 1 summarizes the properties of the actuator and biological muscles. The coil actuator showed strain comparable to that of typical biological muscles, although the stress was much smaller than that of such muscles. The apparent density, which is the mass of the coil divided by the volume of a circular column circumscribing the coil, was small, indicating that the actuator was light. The strain rate was not very slow compared to that of typical biological muscles. The modulus, which was calculated using the spring constant of the coil (9.4 μN mm^{-1}, see Figure S6 in the Supporting Information), was considerably smaller than that of biological muscles. Because the coil actuators were made of silicone, they seemed to be applicable in the field of miniaturized soft robotics in biomedical applications.

Table 1. Properties of the Silicone Coil Actuators and Biological Muscles

property	silicone coil actuator	biological muscle
strain (%)	54	50[a]
stress (kPa)	1.2	500[a]
apparent density (g cm^{-3})	0.09[b]	∼1[c]
strain rate (% s^{-1})	7.7	>50[c]
modulus (MPa)	10−60[c]	6.5 × 10^{-5}[b]

[a]Reference 29. [b]The density and modulus were calculated from a circular column circumscribing the coil. [c]Reference 30.

In biological applications, the ability to resist acidic and basic environments is important. This ability was tested as follows. At room temperature, the silicone coils were immersed in aqueous solutions of hydrochloric acid and sodium hydroxide for 24 h. Then, the coils were washed with distilled water and observed using a digital microscope (Figure S7). In the acidic environment, the coil shape was retained, although moderate deformation was observed. Pitches were increased by 19 and 26% for 1 M HCl and pH 3 solutions, respectively. In the basic environment with pH 11, the pitch was increased by 63%, indicating that the coils were more unstable under basic conditions. Thus, the coil shape was retained under normal biological conditions, although it was moderately deformed. However, in a 1 M sodium hydroxide solution, complete uncoiling occurred, suggesting that the silica-like layer formed by UV−ozone treatment was dissolved in a strongly basic solution.

CONCLUSION

Silicone strings with a diameter of 140 μm were prepared by solidifying the silicone prepolymer inside a glass capillary. The strings were transformed to microcoils through oxidation by UV−ozone treatment while the string was prestretched and pretwisted. The oxidized portion faced outward, as confirmed by coil staining. The pitch and diameter of the coils were controlled by the pretwisting angles, which were also understood using geometrical considerations. Because the inner diameter of glass capillaries can be reduced to submicrometer size with current technologies,[31] in the future, the size of the coils is expected to be much smaller than those demonstrated herein. As an application of the coils, an actuator with a large strain was prepared, which could repeatedly transform from a coil to a straight shape using swelling/

https://doi.org/10.1021/acsomega.2c00475
ACS Omega 2022, 7, 11363−11370

deswelling with hexane. Thus, actuators with a coil shape exhibit a large stroke. Silicone was used as a highly biocompatible material. Therefore, the coil is expected to be used in the biomedical microrobotics field in the future. Although the material used in this study was a composite of zinc oxide powder in a silicone matrix, various functionalities, such as the electrical conductivity and magnetic field response, are expected when other powder materials are used.[32,33]

■ ASSOCIATED CONTENT

Supporting Information

The Supporting Information is available free of charge at https://pubs.acs.org/doi/10.1021/acsomega.2c00475.

Experimental apparatus; optical images of coils with various string diameters; relationship between the curvature of silicone strings and the duration of UV−ozone treatment; optical images of coils prepared using transparent silicone; optical image of a polyurethane coil; schematic of the measurement method for spring constants; and optical images of coils before and after immersion in aqueous solutions (PDF)

■ AUTHOR INFORMATION

Corresponding Author

Masashi Watanabe − *Faculty of Textile Science and Technology, Shinshu University, Ueda, Nagano 386-8567, Japan*; orcid.org/0000-0001-5995-8019; Email: mwatana@shinshu-u.ac.jp

Authors

Toshiki Tokutake − *Faculty of Textile Science and Technology, Shinshu University, Ueda, Nagano 386-8567, Japan*

Ai Harada − *Faculty of Textile Science and Technology, Shinshu University, Ueda, Nagano 386-8567, Japan*

Masatoshi Kaminaga − *Faculty of Textile Science and Technology, Shinshu University, Ueda, Nagano 386-8567, Japan*

Complete contact information is available at: https://pubs.acs.org/10.1021/acsomega.2c00475

Notes

The authors declare no competing financial interest.

■ ACKNOWLEDGMENTS

This work was supported by JSPS KAKENHI (grant number 20K05630).

■ REFERENCES

(1) Schurch, P.; Ramachandramoorthy, R.; Petho, L.; Michler, J.; Philippe, L. Additive Manufacturing by Template-Assisted 3D Electrodeposition: Nanocrystalline Nickel Microsprings and Microspring Arrays. *Appl. Mater. Today* **2020**, *18*, 100472.

(2) Iamsaard, S.; Asshoff, S. J.; Matt, B.; Kudernac, T.; Cornelissen, J. J. L. M.; Fletcher, S. P.; Katsonis, N. Conversion of Light into Macroscopic Helical Motion. *Nat. Chem.* **2014**, *6*, 229−235.

(3) Phan, P. T.; Hoang, T. T.; Thai, M. T.; Low, H.; Lovell, N. H.; Do, T. N. Twisting and Braiding Fluid-Driven Soft Artificial Muscle Fibers for Robotic Applications. *Soft Robot.*, published online Oct 5, 2021, DOI: 10.1089/soro.2021.0040.

(4) Li, W.; Huang, G.; Wang, J.; Yu, Y.; Wu, X.; Cui, X.; Mei, Y. Superelastic Metal Microsprings as Fluidic Sensors and Actuators. *Lab Chip* **2012**, *12*, 2322−2328.

(5) Choi, K.; Park, S. J.; Won, M.; Park, C. H. Soft Inductive Coil Spring Strain Sensor Integrated with SMA Spring Bundle Actuator. *Sensors* **2021**, *21*, 2304.

(6) Xu, F.; Lu, W.; Zhu, Y. Controlled 3D Buckling of Silicon Nanowires for Stretchable Electronics. *ACS Nano* **2011**, *5*, 672−678.

(7) Kim, H.-J.; Kim, S.-H.; Park, S. Effects of the Carbon Fiber-Carbon Microcoil Hybrid Formation on the Effectiveness of Electromagnetic Wave Shielding on Carbon Fibers-Based Fabrics. *Materials* **2018**, *11*, 2344.

(8) Liu, S.; Deng, J.; Zeng, B.; Jia, Y. Embolization with Microcoils for Urethral Hemorrhage A Case Report. *Medicine* **2019**, *98*, e16184.

(9) Huang, T.; Liu, Z.; Huang, G.; Liu, R.; Mei, Y. Grating-Structured Metallic Microsprings. *Nanoscale* **2014**, *6*, 9428−9435.

(10) Antartis, D. A.; Mott, R. N.; Chasiotis, I. Silicon Nanosprings Fabricated by Glancing Angle Deposition for Ultra-Compliant Films and Interfaces. *Mater. Des.* **2018**, *144*, 182−191.

(11) Motojima, S.; Chen, X.; Yang, S.; Hasegawa, M. Properties and Potential Applications of Carbon Microcoils/Nanocoils. *Diam. Relat. Mater.* **2004**, *13*, 1989−1992.

(12) Ushiba, S.; Masui, K.; Taguchi, N.; Hamano, T.; Kawata, S.; Shoji, S. Size Dependent Nanomechanics of Coil Spring Shaped Polymer Nanowires. *Sci. Rep.* **2015**, *5*, 17152.

(13) Iwaki, M.; Wickham, S. F.; Ikezaki, K.; Yanagida, T.; Shih, W. M. A Programmable DNA Origami Nanospring That Reveals Force-Induced Adjacent Binding of Myosin VI Heads. *Nat. Commun.* **2016**, *7*, 13715.

(14) Kamata, K.; Piao, Z.; Suzuki, S.; Fujimori, T.; Tajiri, W.; Nagai, K.; Iyoda, T.; Yamada, A.; Hayakawa, T.; Ishiwara, M.; Horaguchi, S.; Belay, A.; Tanaka, T.; Takano, K.; Hangyo, M. Spirulina-Templated Metal Microcoils with Controlled Helical Structures for THz Electromagnetic Responses. *Sci. Rep.* **2015**, *4*, 4919.

(15) Li, B.; Gil, B.; Power, M.; Gao, A.; Treratanakulchai, S.; Anastasova, S.; Yang, G.-Z. Carbon-Nanotube-Coated 3D Microspring Force Sensor for Medical Applications. *ACS Appl. Mater. Interfaces* **2019**, *11*, 35577−35586.

(16) Yu, Y.; Shang, L.; Gao, W.; Zhao, Z.; Wang, H.; Zhao, Y. Microfluidic Lithography of Bioinspired Helical Micromotors. *Angew. Chem., Int. Ed.* **2017**, *56*, 12127−12131.

(17) Yoshida, K.; Nakajima, S.; Kawano, R.; Onoe, H. Spring-Shaped Stimuli-Responsive Hydrogel Actuator with Large Deformation. *Sens. Actuators B* **2018**, *272*, 361−368.

(18) Kanik, M.; Orguc, S.; Varnavides, G.; Kim, J.; Benavides, T.; Gonzalez, D.; Akintilo, T.; Tasan, C. C.; Chandrakasan, A. P.; Fink, Y.; Anikeeva, P. Strain-Programmable Fiber-Based Artificial Muscle. *Science* **2019**, *365*, 145−150.

(19) Wu, Z. L.; Moshe, M.; Greener, J.; Therien-Aubin, H.; Nie, Z.; Sharon, E.; Kumacheva, E. Three-Dimensional Shape Transformations of Hydrogel Sheets Induced by Small-Scale Modulation of Internal Stresses. *Nat. Commun.* **2013**, *4*, 1586.

(20) Chen, Z.; Linghu, C.; Yu, K.; Zhu, J.; Luo, H.; Qian, C.; Chen, Y.; Du, Y.; Zhang, S.; Song, J. Fast Digital Patterning of Surface Topography toward Three-Dimensional Shape-Changing Structures. *ACS Appl. Mater. Interfaces* **2019**, *11*, 48412−48418.

(21) Obata, K.; Slobin, S.; Schonewille, A.; Hohnholz, A.; Unger, C.; Koch, J.; Suttmann, O.; Overmeyer, L. UV Laser Direct Writing of 2D/3D Structures Using Photo-Curable Polydimethylsiloxane (PDMS). *Appl. Phys. A: Mater. Sci. Process.* **2017**, *123*, 495.

(22) Efimenko, K.; Wallace, W. E.; Genzer, J. Surface Modification of Sylgard-184 Poly(Dimethyl Siloxane) Networks by Ultraviolet and Ultraviolet/Ozone Treatment. *J. Colloid Interface Sci.* **2002**, *254*, 306−315.

(23) Watanabe, M.; Mizukami, K. Well-Ordered Wrinkling Patterns on Chemically Oxidized Poly(dimethylsiloxane) Surfaces. *Macromolecules* **2012**, *45*, 7128−7134.

(24) del Campo, A.; Nogales, A.; Ezquerra, T. A.; Rodriguez-Hernandez, J. Modification of Poly(Dimethylsiloxane) as a Basis for Surface Wrinkle Formation: Chemical and Mechanical Characterization. *Polymer* **2016**, *98*, 327−335.

(25) Yesildag, C.; Tyushina, A.; Lensen, M. Nano-Contact Transfer with Gold Nanoparticles on PEG Hydrogels and Using Wrinkled PDMS-Stamps. *Polymers* **2017**, *9*, 199.
(26) Vig, J. R. Ultraviolet-Ozone Cleaning of Semiconductor Surfaces. In *Handbook of Semiconductor Wafer Cleaning Technology: Science, Technology, and Applications*; Kern, W., Ed.; Noyes: Park Ridge, 1993; Chapter 6.
(27) Graubner, V. M.; Jordan, R.; Nuyken, O.; Schnyder, B.; Lippert, T.; Kotz, R.; Wokaun, A. Photochemical Modification of Cross-Linked Poly(dimethylsiloxane) by Irradiation at 172 nm. *Macromolecules* **2004**, *37*, 5936−5943.
(28) Ma, C.; Lu, W.; Yang, X.; He, J.; Le, X.; Wang, L.; Zhang, J.; Serpe, M. J.; Huang, Y.; Chen, T. Bioinspired Anisotropic Hydrogel Actuators with On-Off Switchable and Color-Tunable Fluorescence Behaviors. *Adv. Funct. Mater.* **2018**, *28*, 1704568.
(29) Wirhed, R. *Anatomi Och Rörelselära Inom Idrotten*; Harpoon Publications AB: Örebro, Sweden, 1984; Chapter 1.
(30) Madden, J. D. W.; Vandesteeg, N. A.; Anquetil, P. A.; Madden, P. G. A.; Takshi, A.; Pytel, R. Z.; Lafontaine, S. R.; Wieringa, P. A.; Hunter, I. W. Artificial Muscle Technology: Physical Principles and Naval Prospects. *IEEE J. Ocean. Eng.* **2004**, *29*, 706−728.
(31) Takami, T.; Iwata, F.; Yamazaki, K.; Son, J. W.; Lee, J.-K.; Park, B. H.; Kawai, T. Direct Observation of Potassium Ions in HeLa Cell with Ion-Selective Nano-Pipette Probe. *J. Appl. Phys.* **2012**, *111*, 044702.
(32) Shabaniverki, S.; Juarez, J. J. Directed Assembly of Particles for Additive Manufacturing of Particle-Polymer Composites. *Micromachines* **2021**, *12*, 935.
(33) Qiao, Y.; Zhang, J.; Zhang, M.; Zhai, P.; Guo, X. Experimental and Modeling Investigations on the Quasi-Static Compression Properties of Isotropic Silicone Rubber-Based Magnetorheological Elastomers under the Magnetic Fields Ranging from Zero to Saturation Field. *Smart Mater. Struct.* **2022**, *31*, 015029.

https://doi.org/10.1021/acsomega.2c00475
ACS Omega 2022, 7, 11363−11370